Electronic Supplementary Material (ESI) for Materials Advances.

Supporting Information

Crystallographic phase changes and damage thresholds of $CsPbI_3$ microwire waveguides through continuous wave photoablation

Kieran O. Russell, [†] Mark A. Osborne[‡] and Aidan A.E. Fisher*[‡]

[†] Department of Chemistry, University of Cambridge, UK

[‡] Department of Chemistry, University of Sussex, Falmer, UK

*Email: correspondence and requests for materials should be addressed to A.A.E.F

(aidan.fisher@sussex.ac.uk)

Methods

Synthetic protocol for $CsPbI_3$ microwires. Cs_2CO_3 (99 %), 1-octadecene (technical grade 90 %) and PbI_2 (98.5 %) were purchased from Alfa Aesar. Oleic acid (technical grade 90 %) and oleylamine (technical grade (70 %) were purchased from Sigma Aldrich.

Cs_2CO_3 (0.614 mmol) was loaded into a single neck round bottom flask with octadecene (10 mL) and oleic acid (1 mL). The flask was heated under vacuum to 150 ^oC until all of the Cs_2CO_3 had dissolved. The temperature was subsequently reduced to 120 ^oC.

PbI_2 (0.188 mmol), oleylamine (0.5 mL) and oleic acid (0.5 mL) were loaded into a two-neck round bottom flask and the temperature raised to 140 ^oC under an inert N_2 atmosphere. After 5 minutes the temperature was raised to 160 ^oC and the cesium oleate precursor (0.5 mL) was injected through a rubber septum.

The reaction mixture was held at temperature for a further 15 minutes after which the flask was allowed to cool to room temperature. The longer growth period of 15 minutes, compared with the literature protocol, may contribute to formation of the yellow δ-phase rather than the PL active phase since the PL active phase of $CsPbI_3$ only remains stable whilst QD size is kept sub-15 nm.[1] Ethanol (5 mL) was used to flocculate the microwires. Interestingly, recent reports suggest that the polar solvent induces self-assembly of nanoparticles into yellow δ-phase microwires and some debate remains regarding the exact growth mechanism.[2] The suspension was separated by centrifugation at 3000 RPM for 30 minutes. The supernatant was discarded and the solid yellow microwire pellet redispersed in hexane.

X-ray diffraction. X-ray diffraction was performed using a Siemens D500 powder diffractometer. Dry powder samples were ground into a powder (800 mg) and loaded onto a zero diffraction plate. Analysis was completed using copper K-alpha radiation at 40 kV and 30 mA. (Supplementary Figure S1) shows the dry yellow microwire powder.

Scanning electron microscope. Samples were diluted in hexane and drop cast on to a copper substrate. Microwires were analysed using a Leica Stereoscan 430 equipped with a back scattered electron (BSE) detector and energy dispersive x-ray detector (EDX) (Oxford instruments). EDX data was processed using the Oxford instruments INCA software.

Transmission electron microscopy. Low-resolution electron microscopy work and tomographic reconstruction was conducted using a JEOL JEM 1400 Plus operating at an accelerating voltage of 125 kV. Images were captured on a 16-bit Gatan OneView CMOS.

Electron tomography was completed using a single axis high tilting sample holder. The tilt series was collected over a ± 50^o range at 2^o increments. The reconstruction process was performed using the ETomo and Tomviz software packages.

High resolution images, high angle annular dark field (HAADF), energy dispersive x-ray (EDX) mapping and micro-diffraction was accomplished using an FEI Technai Osiris S/TEM instrument operating at 200 kV. The instrument was equipped with a field assisted thermionic emission source (extreme Schottky XFEG gun) capable of delivering currents of up to 50 nA. Characteristic x-rays were detected

using the FEI super-x geometry across 4 silicon drift detectors. Spectrum images were acquired using a probe current of 0.7 nA at 200 kV and a 200 ms/pixel dwell time. EDX mapping was processed using the FEI super-x software. Images were collected on a Gatan UltraScan 1000XP camera. All micro diffraction measurements were performed using a camera length of 115 mm.

UV-Vis spectroscopy. Samples were diluted in hexane and pipetted into UV fused quartz cuvettes for analysis. Data was acquired using a Perkin Elmer Lambda 265 spectrometer using a Xenon flash source lamp. Data was averaged over a total of 5 scans.

Optical microscopy and ablation. Laser excitation: illumination of the microwires was performed using an inverted optical microscope (Nikon/TE2000/Japan) with through objective illumination. We employed a total of 5 different laser illumination wavelengths (405/448/473/532 and 561 nm), where all lasers operated as continuous wave lasers and produced a TEM_{00} beam profile. Kinematic mirrors were employed to direct the laser light through a Fresnel rhomb and finally into the rear of the microscope. Laser light was directed into the back aperture of the objective lens (Nikon/100 × 1.40 NA/Japan) using a dichroic mirror (Semrock/496 long-pass, Di01 R405/488/532/635 or Di01 R488/561/USA) and focussed to a diffraction-limited spot. The motorised sample stage (Prior/HF110/UK) was controlled using a central hub (Prior/Proscan II/UK).

Samples dispersed in hexane were spin coated (3000 RPM) on to coverslips (Menzel Glaser/24 × 50/0.13 mm) for ablation statistics studies.

Dilute samples in hexane were drop cast on to lacey carbon copper grids (Agar Scientific/400 mesh) for electron microscopy ablation studies. The lacey carbon grids were supported on a clean coverslip and laser ablation performed directly through the lacey carbon grid.

Brightfield images were collected by viewing through the eyepiece using a smartphone. A fibre optic coupled to a spectrometer (CNI/Firefly-4000/China) was connected to the microscope viewing port for wavelength analysis measurements.

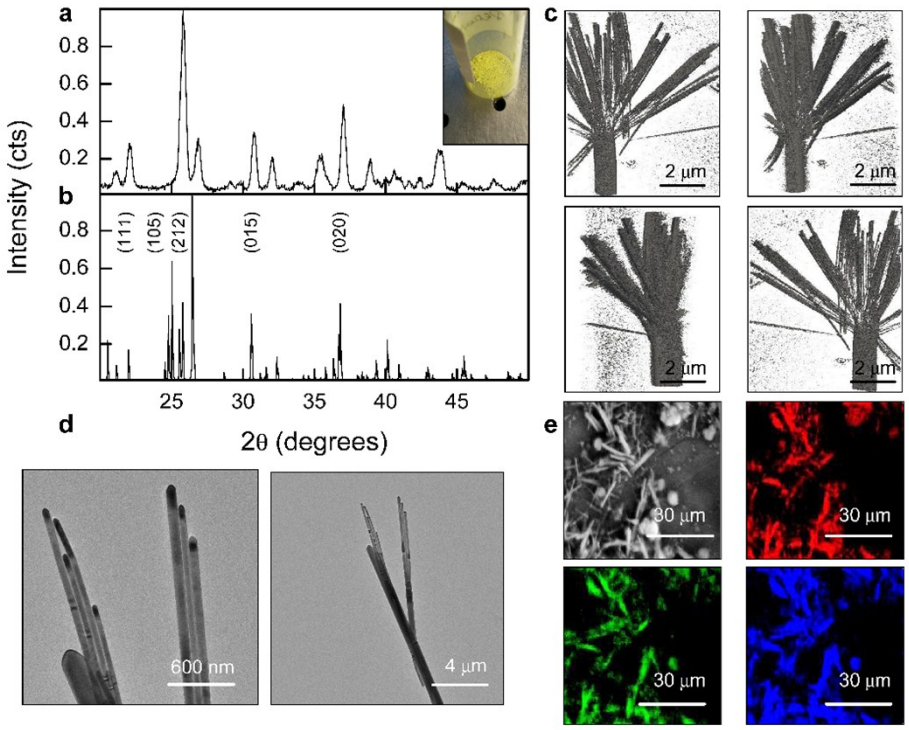

Fig S1. (a) Experimental XRD pattern with image of the microwire powder (inset). (b) Simulated XRD pattern (ICSD: 027979) with prominent peaks of the yellow δ-phase (Pnma No.62) indexed. (c) Tomographic reconstruction of a single microwire tip viewed from various directions about the z-axis. (d) Brightfield low-resolution images of the microwire tips highlighting the divergent growth and the segregation of the macrostructure into smaller microwires. (e) SEM image of the microwire (top-left). Elemental analysis of the microwires (red = Pb Lα), (green = Cs Lα) and (blue = I Lα). The atomic ratios were calculated as Cs:Pb:I = 1:1.1:3 consistent with the expected stoichiometry.

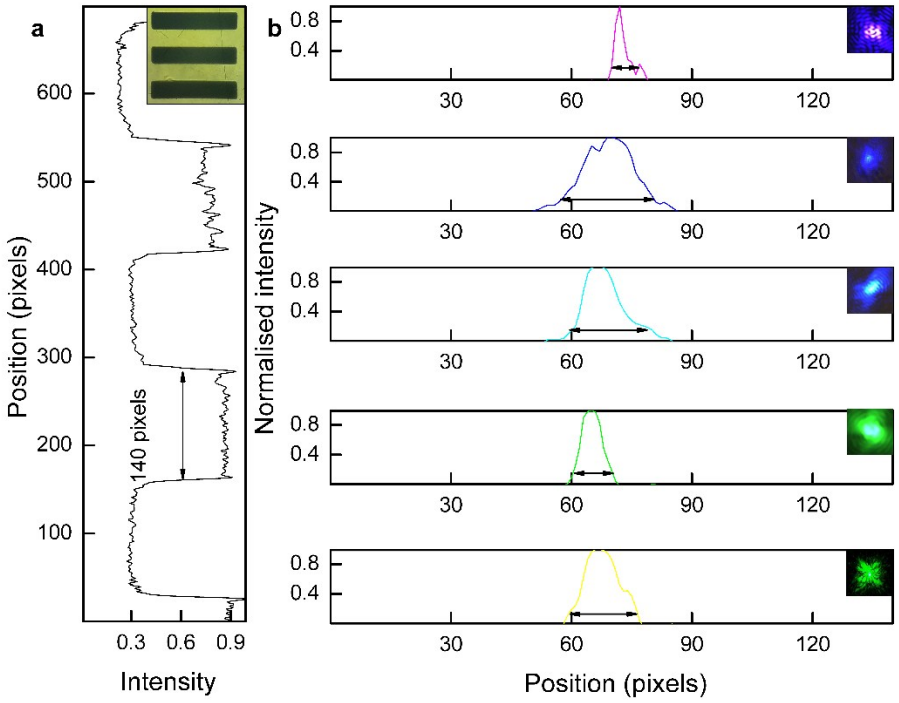

Fig S2. (a) Line profile of the 1951 USAF resolution chart (inset) group 5 element 1. This yields a pixel size of about 63 nm/pixel. (b) Line profiles of the near-Gaussian beams for each laser wavelength focussed to a diffraction limited spot. The insets show the typical beam profile for each wavelength employed (405 to 561 nm top to bottom). We define the beam diameter using the $1/e^2$ definition, which is indicated by the double headed arrow in each laser profile. The diameters given here were used to estimate laser power intensities in the main paper. The beam diameters, using the $1/e^2$ definition, were estimated as (405 = 0.6 μm), (447 = 1.3 μm), (473 = 1.2 μm), (532 = 0.9 μm), (561 = 1.3 μm).

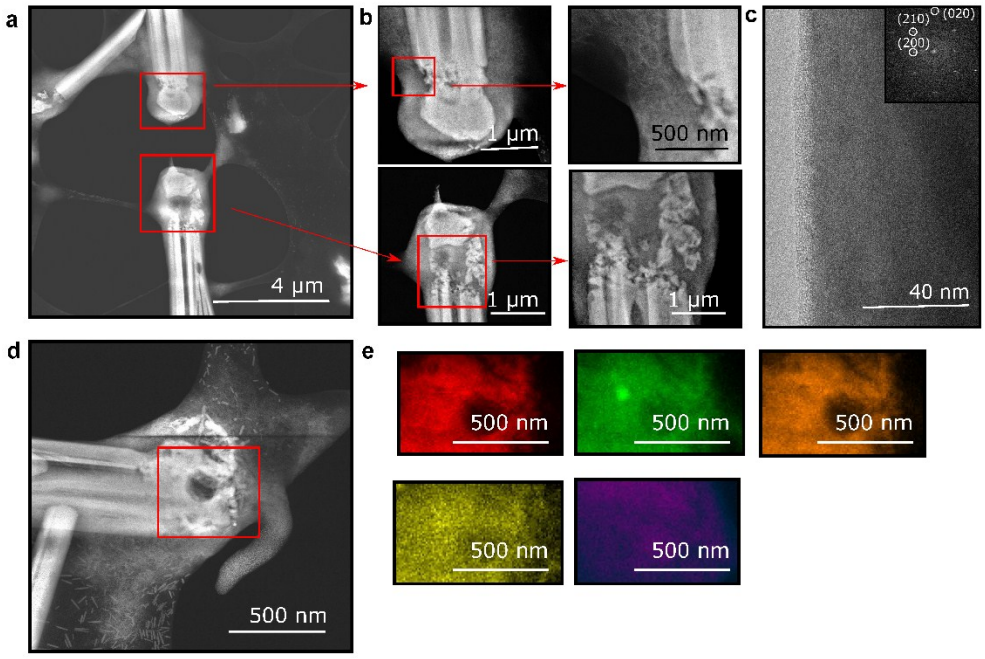

Fig S3. (a) High angle annular dark field (HAADF) of a single microwire, which has been cleaved in two. (b) Magnified images of the regions indicated. We find a low contrast shell around the microwire head which is amorphous and is likely organic residue and organic surface ligand. (c) High resolution image of the non-photoablated MW. Inset shows the corresponding FFT indexed as the yellow δ-phase (Pnma No.62) lattice. (d) HAADF of a microwire tip. Above and below the ablation region indicated by the red box we find sub-100 nm fragments of the microwire deposited on to the lacey carbon grid. (e) Elemental mapping of the area indicated in (d). Here (red = I Lα), (green = Pb Mα), (orange = Cs Lα), (yellow = Si Kα) and (purple = C Kα). We postulate that the silicon present arises from the glass substrate on which the ablation is performed.

References

(1) Protesescu, L.; Yakunin, S.; Bodnarchuk, M. I.; Krieg, F.; Caputo, R.; Hendon, C. H.; Yang, R. X.; Walsh, A.; Kovalenko, M. V. Nanocrystals of cesium lead halide perovskites (CsPbX3, X= Cl, Br, and I): novel optoelectronic materials showing bright emission with wide color gamut. *Nano Lett.* **2015,** *15* (6), 3692.

(2) Sun, J.-K.; Huang, S.; Liu, X.-Z.; Xu, Q.; Zhang, Q.-H.; Jiang, W.-J.; Xue, D.-J.; Xu, J.-C.; Ma, J.-Y.; Ding, J.et al. Polar Solvent Induced Lattice Distortion of Cubic CsPbI3 Nanocubes and Hierarchical Self-Assembly into Orthorhombic Single-Crystalline Nanowires. *Journal of the American Chemical Society* **2018,** *140* (37), 11705.